





3 | Environmental Microbiology | Research Article

# Metabologenomics reveals strain-level genetic and chemical diversity of *Microcystis* secondary metabolism

Colleen E. Yancey,<sup>1</sup> Lauren Hart,<sup>2,3</sup> Sierra Hefferan,<sup>2,4</sup> Osama G. Mohamed,<sup>3,5,6</sup> Sean A. Newmister,<sup>3</sup> Ashootosh Tripathi,<sup>3,5,6</sup> David H. Sherman,<sup>3,4,6</sup> Gregory J. Dick<sup>1,2,7</sup>

**AUTHOR AFFILIATIONS** See affiliation list on p. 16.

**ABSTRACT** *Microcystis* spp. are renowned for producing the hepatotoxin microcystin in freshwater cyanobacterial harmful algal blooms around the world, threatening drinking water supplies and public and environmental health. However, Microcystis genomes also harbor numerous biosynthetic gene clusters (BGCs) encoding the biosynthesis of other secondary metabolites, including many with toxic properties. Most of these BGCs are uncharacterized and currently lack links to biosynthesis products. However, recent field studies show that many of these BGCs are abundant and transcriptionally active in natural communities, suggesting potentially important yet unknown roles in bloom ecology and water quality. Here, we analyzed 21 xenic Microcystis cultures isolated from western Lake Erie to investigate the diversity of the biosynthetic potential of this genus. Through metabologenomic and in silico approaches, we show that these Microcystis strains contain variable BGCs, previously observed in natural populations, and encode distinct metabolomes across cultures. Additionally, we find that the majority of metabolites and gene clusters are uncharacterized, highlighting our limited understanding of the chemical repertoire of Microcystis spp. Due to the complex metabolomes observed in culture, which contain a wealth of diverse congeners as well as unknown metabolites, these results underscore the need to deeply explore and identify secondary metabolites produced by Microcystis beyond microcystins to assess their impacts on human and environmental health.

**IMPORTANCE** The genus *Microcystis* forms dense cyanobacterial harmful algal blooms (cyanoHABs) and can produce the toxin microcystin, which has been responsible for drinking water crises around the world. While microcystins are of great concern, *Microcystis* also produces an abundance of other secondary metabolites that may be of interest due to their potential for toxicity, ecological importance, or pharmaceutical applications. In this study, we combine genomic and metabolomic approaches to study the genes responsible for the biosynthesis of secondary metabolites as well as the chemical diversity of produced metabolites in *Microcystis* strains from the Western Lake Erie Culture Collection. This unique collection comprises *Microcystis* strains that were directly isolated from western Lake Erie, which experiences substantial cyanoHAB events annually and has had negative impacts on drinking water, tourism, and industry.

**KEYWORDS** cyanoHABs, secondary metabolism, *Microcystis*, metabologenomics, natural products

The cyanobacterium *Microcystis aeruginosa* threatens freshwater systems around the world (1, 2) as it regularly dominates cyanobacterial harmful algal blooms (cyano-HABs) and produces a wide range of secondary metabolites (Fig. S1)—with a range of toxic properties (3–5). CyanoHABs are expected to intensify with climate change through increased temperatures, rising atmospheric carbon dioxide concentrations, and

**Editor** Justin J. J. van der Hooft, Wageningen University, Wageningen, the Netherlands

Address correspondence to Gregory J. Dick, adick@umich.edu.

C.E.Y. was a graduate student at the time this research was completed but is now an employee at New England Biolabs, Ipswich, MA, USA.

See the funding table on p. 16.

Received 8 March 2024 Accepted 22 April 2024 Published 25 June 2024

This is CIGLR Contribution Number 1235.

Copyright © 2024 Yancey et al. This is an openaccess article distributed under the terms of the Creative Commons Attribution 4.0 International license.

exacerbation of anthropogenic nutrient pollution by extreme weather events (6–8). Some studies suggest that these conditions will favor more toxic cyanobacteria in future blooms (9–11). CyanoHABs pose threats to tourism, industry, access to potable water, and environmental and human health. Thus, it is critical to assess and monitor the threats of cyanoHABs under varying environmental conditions.

Microcystis spp. receive much attention for their production of the hepatotoxin microcystin (12, 13), which has led to several drinking water crises in both developed and developing nations (14-16), livestock poisoning and death (17), and human illness (18, 19). The vast majority of research on cyanobacterial secondary metabolism is devoted to the study of microcystins, which make up over 90% of the published literature (20). However, several novel cyanobacterial metabolite classes and their associated gene clusters have been discovered recently (21, 22), highlighting our limited understanding of their biosynthetic potential. Furthermore, Microcystis has complex genomes (23, 24) containing numerous biosynthetic gene clusters (BGCs) that may produce a diverse arsenal of secondary metabolites that are highly varied among species and strains (23-26). Many of these previously described secondary metabolites have toxic properties, which may have greater potency when produced in combination, and have been detected in drinking water sources (3, 20, 27-29). While some studies have characterized BGCs present in Microcystis strains (5, 25, 26) and others have resolved the structure and formula of metabolites including microcystins, aeruginosins, cyanopeptolins, and microviridins (30-35), studies that integrate genomic and metabolomic approaches to link genotype and chemical phenotype are lacking. As a result, our understanding of Microcystis secondary metabolism beyond microcystin and a few other cyanopeptides with toxic properties remains limited.

Western Lake Erie (WLE) is a critical source of freshwater for both the United States and Canada. CyanoHABs have become an increasing threat to WLE over the past 30 years as *Microcystis* dominates blooms on an annual basis (36–38). Current routine monitoring for four cyanotoxins in WLE includes microcystin, anatoxin-a, cylindrospermopsin, and saxitoxin (39). While these monitoring strategies are more extensive than in most freshwater systems, they may miss other potentially harmful secondary metabolites produced by *Microcystis* as evidenced by the abundance of transcriptionally active BGCs in natural WLE populations (26). Therefore, it is critical to deeply examine the secondary metabolite potential of *Microcystis* to define the extent of metabolite diversity and potential toxicity.

In this study, we leverage the Western Lake Erie Culture Collection (WLECC) (40) to better understand the repertoire of known and novel BGCs and secondary metabolites in various strains of *Microcystis* that comprise natural populations in WLE. Previously, the only cultivated and publicly available strain of *M. aeruginosa* isolated from WLE was LE-3 (41), which was isolated over 20 years ago. The WLECC is ideal for targeted WLE studies as it contains strains with various biosynthetic genotypes that were exclusively isolated from this location (40). Here, we deeply annotate BGCs encoding secondary metabolites, implement chemical profiling approaches to qualitatively assess chemical diversity produced in culture, and putatively link BGCs and metabolites via computational approaches to better understand the secondary metabolism of *Microcystis*.

## **RESULTS**

#### Overview of WLE microcystis strain biosynthetic capacity

Genomic analysis showed that the WLE *Microcystis* strains contained diverse BGCs that encode multiple enzyme classes including nonribosomal peptides synthases (NRPSs), polyketide synthases (PKSs), hybrid NRPS-PKS modules, and ribosomally synthesized and post-translationally modified (RiPP) peptides. Of the 21 strains examined (Table S1), only five contained the complete *mcy* operon, which produces microcystin (Fig. 1), while two strains contained the partial *mcy* operon (42). Ten isolates contained complete BGCs thought to encode aeruginosins (*aer*), while 11 contained cyanopeptolin-encoding gene clusters (*mcn*). The *apn* operon, which encodes the biosynthesis of anabaenopeptins,

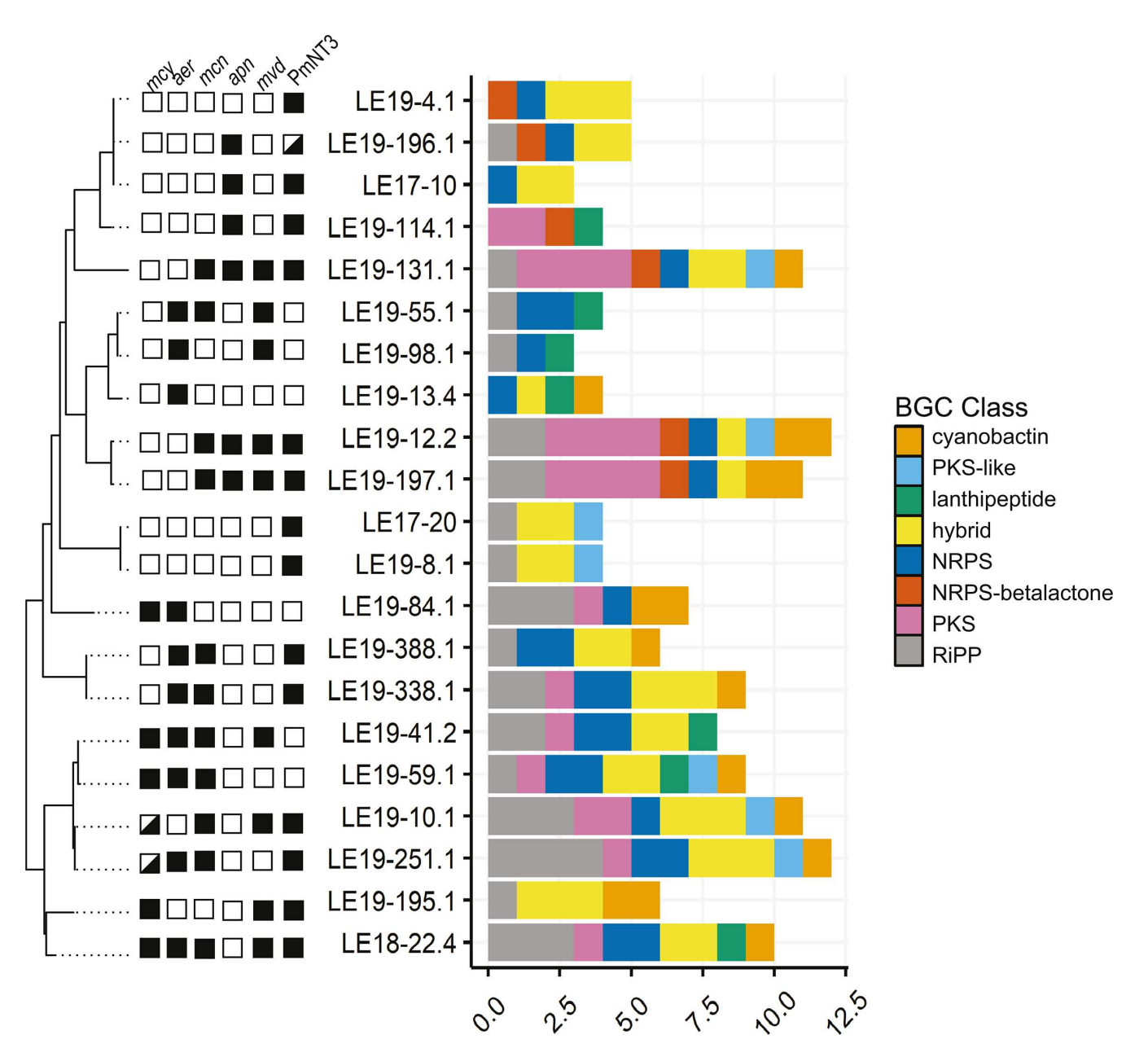


FIG 1 Overview of BGCs in WLE *Microcystis* culture isolates. A phylogenetic tree based on concatenated universal single-copy genes, of the *Microcystis* isolates in the WLECC, as previously described by Yancey et al. (43). Colored boxes indicate that the presence or absence of common *Microcystis* secondary metabolite genes includes the *mcy* (microcystin), *aer* (aeruginosin), *mcn* (cyanopeptolin/micropeptin), *apn* (anabaenopeptin), and *mvd* (microviridin B) operons, as well as the BGC, PmNT3, which may encode the biosynthesis of a paracyclophane molecule. The bar graph indicates the putative count and broad classification of BGCs within each *Microcystis* genome.

was detected in six strains, while *mvd* genes encoding microviridins were identified in nine strains. These findings are consistent with previous results based on marker gene analysis (40). BGCs for microcystin, aeruginosin, or cyanopeptolin co-occurred in nine strains, while microviridin and an uncharacterized BGC containing two <u>modular PKSs</u>, an <u>NRPS-like</u>, and a <u>T3PKS</u> (PmNT3) encoding genes showed a more variable distribution among strains. Notably, strains with fewer NRPS or hybrid gene clusters were enriched in PKS and RiPP gene clusters. While BGC composition was relatively conserved within the deepest branches of the phylogenetic tree based on single-copy conserved genes (for

example, LE17-20 and LE19-8.1), the count and type of BGCs varied within some clades (Fig. 1). Detailed gene annotations for each BGC are described in Table S2.

We next investigated the relatedness of BGCs through the generation of gene cluster families (GCFs). We also included BGC sequences obtained from ten 2014 WLE cyanoHAB metagenomes (26) and sequences deposited onto the Minimum Information about a Biosynthetic Gene Cluster (MIBiG) (44), which contains BGCs with confirmed biosynthetic products. Clustering revealed that some GCFs contained BGCs known to encode the biosynthesis of cyanopeptolin/micropeptin, aeruginosin, anabaenopeptin, microcystin, and microviridin B (30, 31, 35, 45–47). GCF networks also illustrated that culture collection BGCs are representative of those observed in the field during the 2014 WLE cyanoHAB but also captured GCFs not identified in those 2014 metagenomes. The majority of GCFs do not contain MiBIG nodes, indicating the lack of previously described associated secondary metabolites (Fig. 2). Detailed GCF trees and cluster schematics for BGCs encoding known *Microcystis* secondary metabolites and uncharacterized PKS clusters are shown in Fig. S2 and S3.

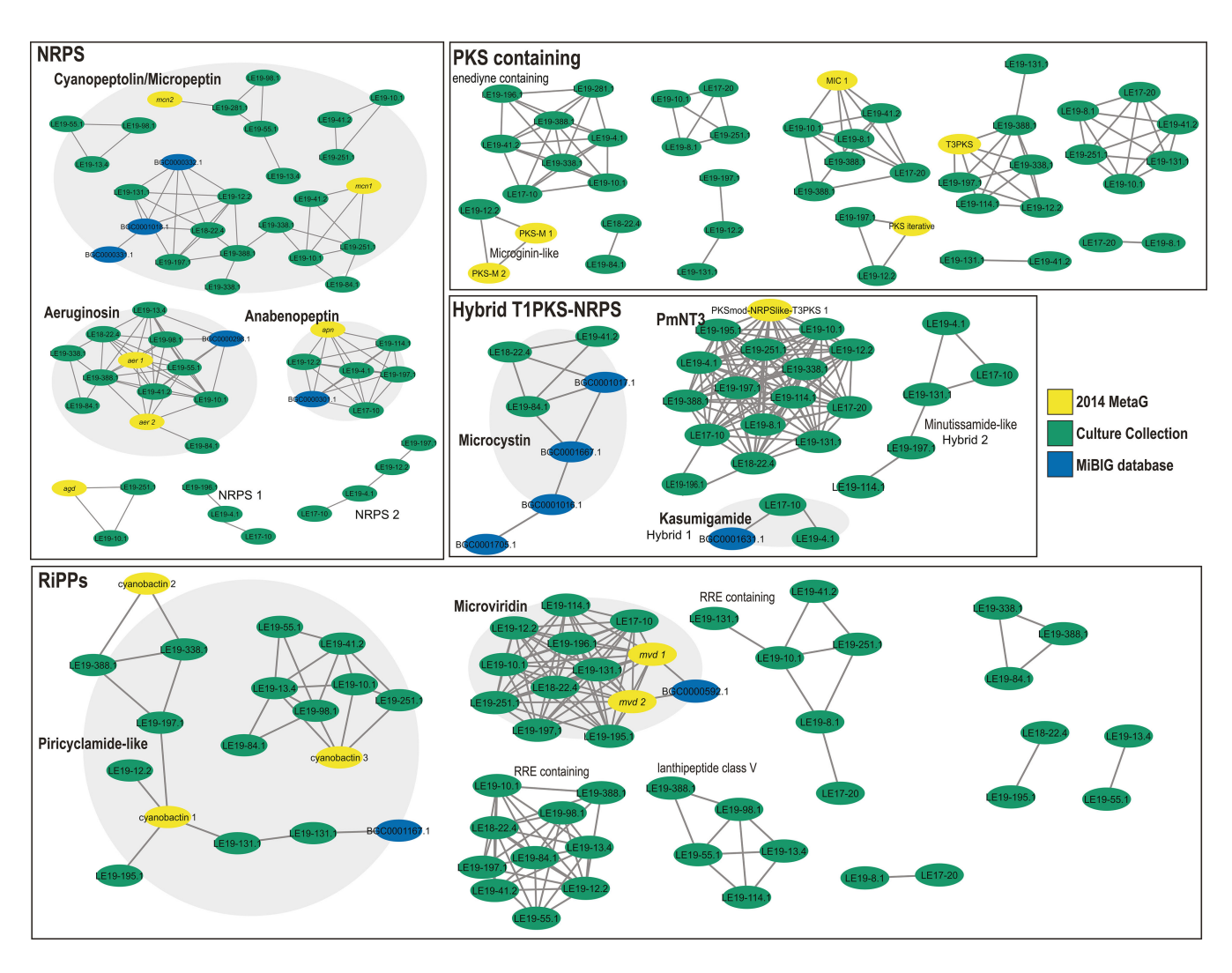


FIG 2 GCFs for Identified BGCs via BiG-SCAPE: Green nodes are from the WLECC, and yellow nodes are from the 2014 WLE cyanoHAB metagenomes. Nodes in purple are from the MiBIG database, which links BGCs with biosynthesis products. Edges between the nodes indicate the similarity of BGCs as calculated through a distance matrix that includes indexes that measure the number of shared PFAM domains, pairs of adjacent PFAM domains, and sequence similarities between predicted protein sequences.

## An unknown BGC with [7,7] paracyclophane biosynthesis potential

An unknown BGC, PmNT3, previously described as an "orphan" BGC in *M. aeruginosa* isolate PCC 7806 (23), was most closely related to BGCs that biosynthesize [7,7] paracyclophanes. This gene cluster, which encodes two modular PKSs, NRPS-like, and T3PKS enzymes, was present in 14 strains and partially present in one strain (LE19-196.1) (Fig. 1 and 3A). This cluster also contained biosynthesis genes that putatively encode an isoprenylcysteine carboxyl methyltransferase and a flavin-binding monooxygenase-like enzyme. Known cluster BLAST analysis (which identifies all genes to closest known BGC from the MiBIG database with significant BLAST hits) revealed 55% similarity to clusters that encode merocyclophane C/D (48), a 41% similarity to cylindrocyclophane D/E/F (49), and a 31% similarity to carbamidocyclophane (50) (Fig. 3B), all of which produce

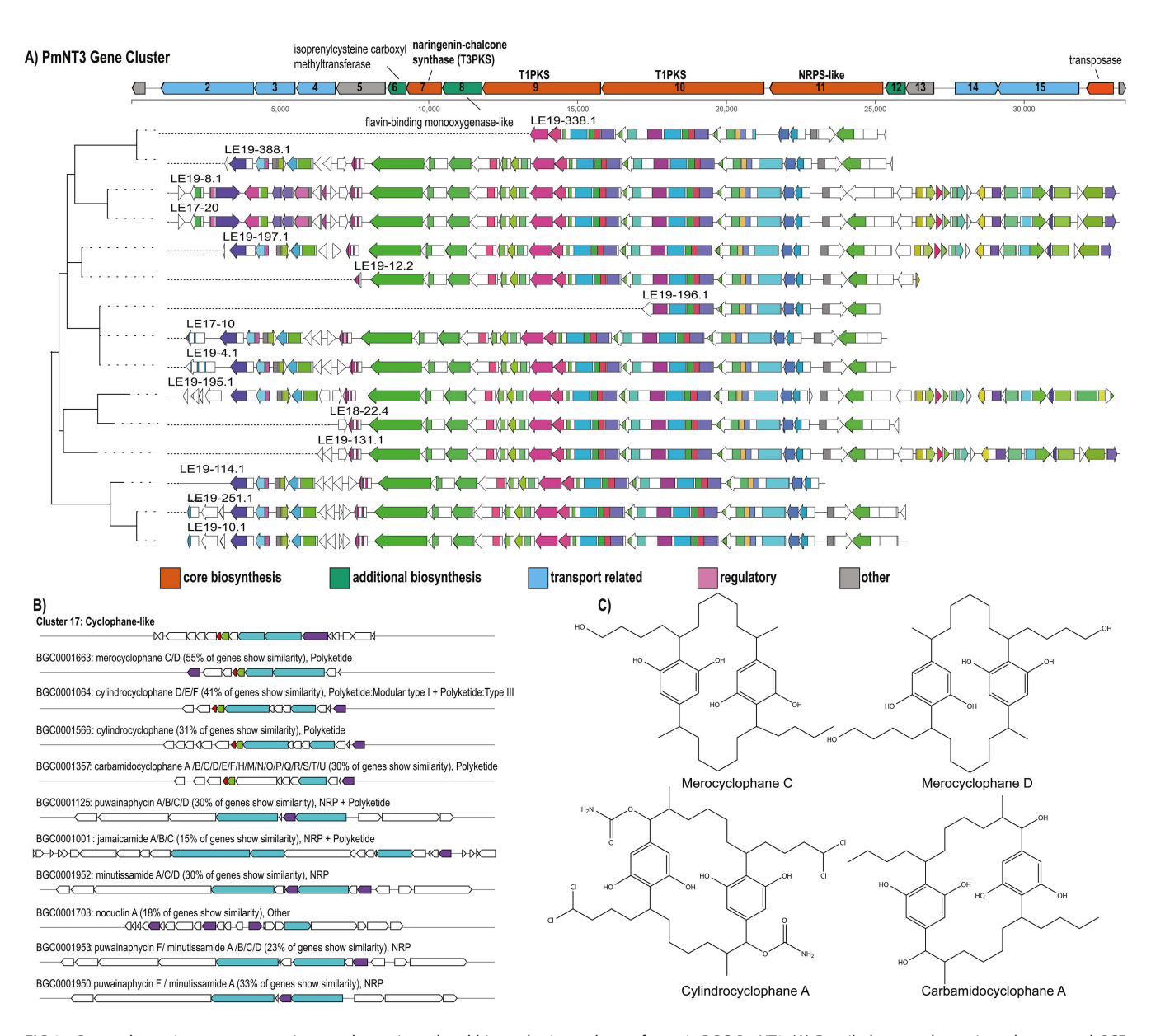


FIG 3 Gene schematics, gene annotations, and putative-related biosynthetic products of cryptic BGC *PmNT3*. (A) Detailed gene schematic and generated GCF tree from antiSMASH and BiG-SCAPE, respectively. Key genes are annotated on the large gene schematic. (B) Known cluster BLAST generated via antiSMASH. The novel BGC shows 30%–55% similarity of gene content to known cyanobacterial BGCs encoding for the biosynthesis of [7, 7] paracyclophanes: merocyclophane C/D (55%), cylindrocyclophane (41%), and carbamidocyclophane (31%). (C) Chemical structures for select cyanobacterial [7, 7] paracyclophanes that are confirmed biosynthesis products from the order *Nostacales*.

cyanobacterial [7,7] paracyclophane molecules (48, 49, 51, 52) (Fig. 3B and C). Genes with similarity hits between PmNT3 and known biosynthesis pathways for [7,7] paracyclophanes included core biosynthesis genes that encode both PKSs, the NRPS-like, T3PKS, and a methyltransferase as determined by antiSMASH (Fig. 3B). Despite its abundance in the WLECC and presence in the 2014 cyanoHAB (Fig. 2), only five publicly available *Microcystis* spp. strains contain this cluster at a 95% identity and query cover: NIES-298, PCC 7806, FACHB-905, PCC 7806SL, and FACHB-1751 (Genbank accessions: CP046058.1, CP020771.1, CP089094.1, AM778955.1, and CP011339.1).

A deeper examination and comparison of this putative gene cluster and the BGC that encodes the biosynthesis of merocyclophane C/D (48) revealed the presence of several conserved and core genes required for [7,7] paracyclophane biosynthesis. PmNT3 11, an NRPS-like encoding gene, shares similar domains and proposed functionality to *merl* and *merA*, which are believed to activate and load the PKS-derived chain. There is high gene sequence similarity (~50%) between the putatively identified T1PKSs in the PmNT3 pathway and T1PKS observed in the *mer* pathway. The T3PKS catalyzes the formation of resorcinol rings, a key step in paracyclophane biosynthesis that has been described for cylindrocylcophane biosynthesis (49). PmNT3 6 and *merF* appear to encode similarly functioning enzymes with carboxyl methyltransferase activity (Table 1). Finally, PmNT3 8 encodes a putative flavin-dependent monooxygenase-like enzyme.

To explore whether this enzyme could be involved in ring closure of the final macrocycle via halogenation and C-C bond formation in a manner analogous to the cylindrocyclophanes (48, 53), a homology model of PmNT3 8 was compared to functionally characterized flavin-dependent halogenases (FDHs) and flavin monooxygenases (FMOs; Fig. S4). This analysis suggested that PmNT3 8 is most likely a monooxygenase (2.1 Ų rmsd AncFMO5, PDB 6SEK). However, high structural homology (3.3 Ų rmsd) with the single-component flavin-dependent halogenase AetF (PDB 8CJF) (54) was also observed. Halogenation of linear alkane substrates by FDH enzymes has not been previously reported, indicating that further studies are required to determine the catalytic function of PmNT3 8.

## Chemical profiling of the WLECC

Chemical profiling by mass spectrometry revealed a diverse metabolome among *Microcystis* isolates in the WLECC. Many chemical features are present in only one to five

TABLE 1 Comparison between merocyclophane encoding BGC (mer) from Nostoc sp. UIC 10110 (NCBI GenBank KY379971.1) and PmNT3

Merocyclophane (mer) gene	Gene from	% identity	% alignment	Identified domains	Proposed function
homolog	WLECC				
merl	PmNT3 11	49	45 (first half)	Co-enzyme A ligase, AMP binding,	Fatty acid co-ligase activation
merA	PmNT3 11	31	8 (at the end)	Acyl-CoA dehydrogenase, and PP binding	and loading of PKS chain (PP binding)
merC	PmNT3 10	48	97	Ketosynthase, acyltransferase, dehydratase, ketoreductase, and PP binding	Installs malonyl-CoA unit and performs full reduction of the ketone to methylene (no alpha methylation like in mer)
merD	PmNT3 9	46	98	Ketosynthase, acyltransferase, dehydratase, ketoreductase, PP binding, and thioesterase	Installation of second malonyl coA unit
merE	PmNT3 7	49	100	NA	Add third malonyl CoA, catalyzes resorcinol ring formation
merF	PmNT3 6	50	93	NA	Isoprenylcysteine carboxyl methyltransferase
NA	PmNT3 8	NA	NA	NA	Flavin-dependent monooxyge- nase-like formation of the final macrocycle

culture isolates (Fig. 4), highlighting highly variable metabolomes across cultures. Most chemical features do not have a spectral match or library analog to chemical structures deposited in the Global Natural Products Social Molecular Networking (GNPS) web server (55), but some putative identifications can be made. For example, several fatty acids, photosynthetic pigment derivatives, and microcystin congeners were annotated with GNPS. Mirror plots and manual annotations for microcystin LR, microcystin YR, and anabaenopeptin NZ857 to known spectral patterns and MS1 m/z values in the cyanometDB (56) provide confidence in the annotation of these cyanopeptides. Common fragmentation patterns are depicted in the manual annotations in all three compounds (Schymanski level 2, Fig. S5). Using additional bioinformatic annotation in silico tools DEREPLICATOR (57) and Structural similarity Network Annotation Platform for Mass Spectrometry (SNAP-MS [58]), we also putatively identified features for anabaenoepeptins, features with high similarity to microginins, and cyanopeptolins/micropeptins (30, 59, 60) (Fig. 4). These annotations are considered level 4 in the Schymanski labeling scheme, limiting our confidence in their actual structure and requiring additional data collection and manual annotation of these metabolites (61). Some chemical features, such as fatty acids and pigment derivatives, were detected often across strains (present in 11 or more cultures), while other features, such as microginin-like metabolites, were rarely detected (i.e., in less than five cultures). This, along with the presence of numerous unique or rare chemical features, highlights the distinct nature of metabolomes across cultures (Fig. 4). Even with the implementation of multiple annotators to facilitate the prediction of structural classes, many chemical features remain unannotated with uncharacterized structure. A complete list of putatively annotated chemical features using GNPS, DEREPLICATOR, and SNAP-MS by culture isolate is shown in Table S3. Of the 68 metabolites putatively annotated, 37 were annotated at level 5 confidence, 28 were at level 4, and 3 were at level 2.

We assessed the presence of a select set of BGCs and their corresponding annotated chemical features or top-scoring candidate features via NPlinker (62) in each culture (Fig. 5). In the case of the *mcy* and *apn* operons, which encode microcystin and anabaenopeptin, respectively, chemical features were annotated with GNPS in most cultures in which the BGC was present. The *aer* cluster was present in 10 cultures, yet there were no annotations for aeruginosin features in any culture (Fig. 5). Similarly, putative annotations

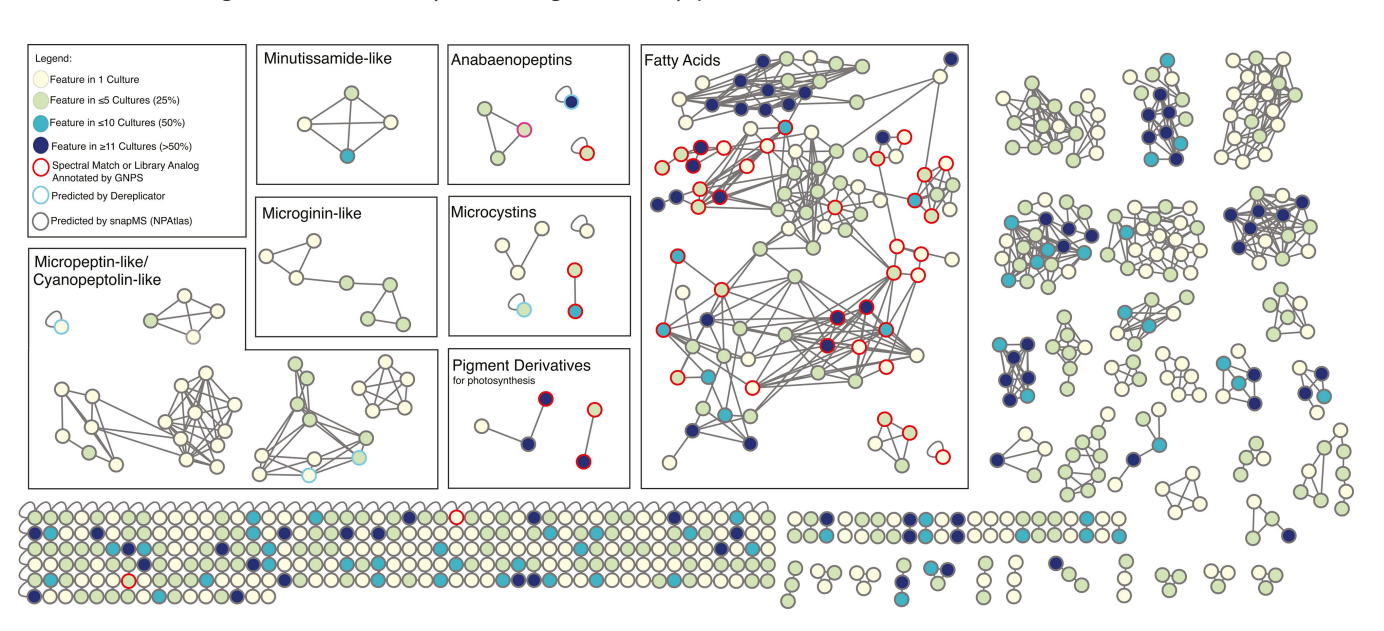


FIG 4 Molecular network representing the WLECC metabolome from positive mode liquid chromatography-mass spectrometry (LC-MS). Nodes are colored based on feature frequency within WLECC cultures (ranging from being found in one culture to all analyzed cultures). Metabolites annotated by GNPS, DEREPLICATOR, and SNAP-MS are outlined in red, light blue, and gray, respectively. Several known *Microcystis* secondary metabolites were putatively identified including microcystins, anabaenopeptins, and features with similarity to micropeptins/cyanopeoptolins, microginins, and minutissamides.

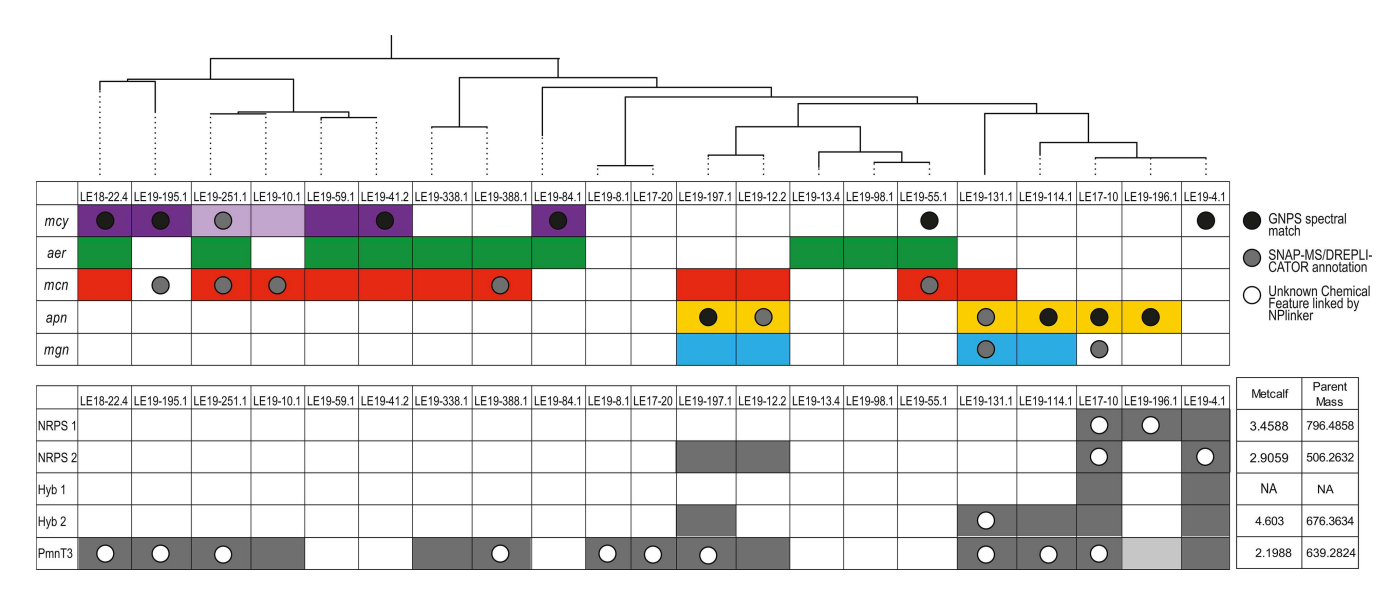


FIG 5 BGC and chemical feature absence matrix for select secondary metabolites: Cultures are arranged based on the phylogenetic tree generated via concatenated single-copy housekeeping genes as described in Yancey et al. (40, 43). On the top matrix, colored boxes indicate the presence of known BGCs (mcy, aer, mcn, apn, and mgn gene clusters). The light purple coloring indicates the presence of the partial mcy operon. Circles indicate the presence of an annotated chemical feature from each culture. Black circles were annotated with GNPS (highest confidence), and gray circles were annotated with either DREPLICATOR or SNAP-MS. On the bottom matrix, colored boxes indicate the presence of cryptic BGCs (annotated in Fig. 2). Gray coloring indicates the presence of core biosynthesis within the PmNT3 cluster in LE19-196.1 White circles indicate the presence of the top-scoring candidate chemical feature with respect to each BGC (NRPS 1, NRPS 2, Hyb1, Hyb 2, and PmNT3), as determined by NPlinker. The Metcalf score and parent mass for top hits are depicted in the box to the right.

for cyanopeptolins/micropeptins were observed in three out of the 11 cultures that contained the *mcn* gene cluster. This result supports the notion that BGCs are not constitutively expressed, and changing environmental conditions or available substrates may influence differential secondary metabolite biosynthesis (63).

For uncharacterized NRPS, hybrid, and PmNT3 clusters (Fig. 2), we also assessed the presence of top-scoring candidate features linked to respective BGCs via NPlinker. The chemical structures of these candidate molecular features are currently unknown. For both the NRPS 1 and 2 GCFs, two cultures with each respective BGC contained the top putatively linked chemical feature (Fig. 5). Of the five strains containing the Hybrid 2 GCF, only one strain contained the top putatively linked chemical feature. For the PmNT3 cluster, 10/14 strains with the complete BGC contained the top putatively linked chemical feature (Fig. 2 and 5). In some cases, microcystins, putatively identified cyanopeptolins/micropeptins, and microginins were annotated in cultures in which the respective BGC was not present (Fig. 5). This may be explained by observed *Microcystis* strain heterogeneity within a few WLECC cultures, in which relative abundance of strains may fluctuate over time during continuous cultivation (40).

## Diversity within cyanopeptolin/micropeptin BGCs and congener identified

Three unique cyanopeptolin/micropeptin-like BGCs were identified in the isolates from this culture collection based on deduplication of sequences (see Materials and Methods, Fig. 6) These clusters were very similar to the *mcn* BGC from isolate *Microcystis* sp. NIVA-CYA (NCBI Genbank: DQ075244.1). Clusters 15 and 4 shared over 97% identity with *mcn* gene cluster from the NIVA-CYA strain, while Cluster 8 was 87% similar. All three WLECC clusters contain a halogenase (*mcnD*), unlike the *mcn* BGC from *M. aeruginosa* K-139 (NCBI Genbank: AB481215.1, Fig. 6B). Putative substituents for features representing micropeptins, specifically features 1,269 and 843, were identified using DEREPLICATOR. Feature 843 shared the *m/z* ratio of 846.47 with micropeptin MZ845, queuing subsequent manual annotation of these spectra. Manual annotation of these spectra verified the identity of this feature with level 2 confidence. Feature 1,269 has an

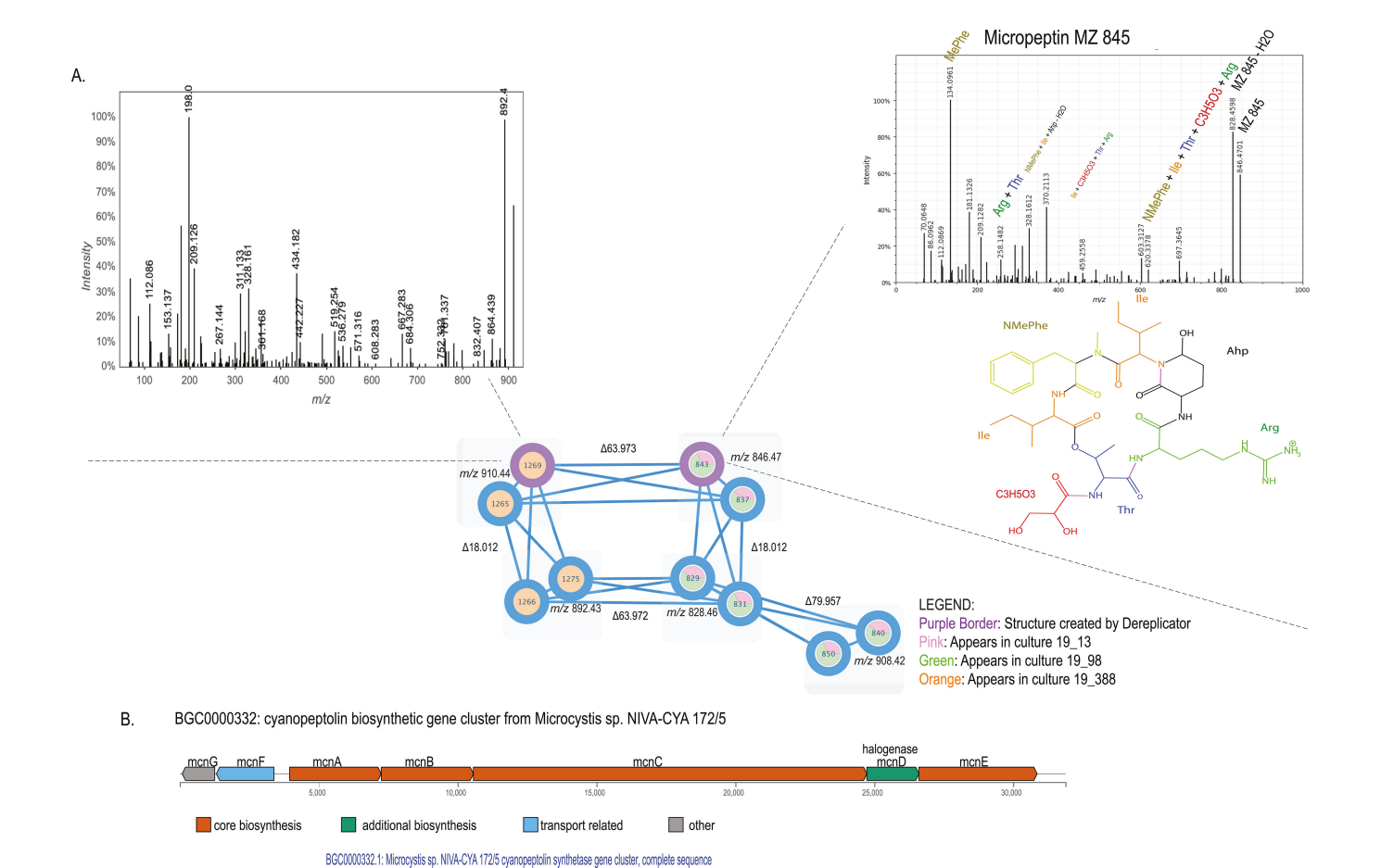


FIG 6 Cyanopeptolin/micropeptin molecular networking and gene cluster analysis. (A) The molecular network with micropeptin cluster was obtained from the WLECC with a cosine similarity score cutoff of 0.70. Nodes are labeled with corresponding cluster index numbers assigned through GNPS, and their *m/z* are shown in black text next to each pair of nodes that share the same *m/z*. Edges between nodes show the mass difference between sets of nodes. Two micropeptins with edges outlined in purple indicate GNPS probable structure detection through GNPS DEREPLICATOR. Pie charts within nodes indicate strains that the metabolites were detected in. Cluster index 843 corresponds to CyanoMetDB micropeptin MZ 845 shown in the figure with the experimental MS/MS [M + H]<sup>+</sup> annotated data shown. Ahp is 3-amino-6-hydroxy-2-piperidone. Cluster index 1,269 had a predicted structure from GNPS DEREPLICATOR but does not correspond to experimental MS/MS data, and the structure remains unidentified. (B) Gene schematics for three gene clusters identified in three WLECC strains, and their comparison to known *mcn* gene clusters deposited in the Minimum Information about a Biosynthetic Gene Cluster (MiBIG) database (https://mibig.secondarymetabolites.org/repository). Genes are colored based on PFAM domain annotation for each cluster.

lacks mcnD, mcnG

MS1 pattern matching micropeptins HU909 and SF909 in CyanoMetDB (56), but isotope signatures verified no chlorine present in the structure, and therefore, the metabolite could not be further annotated with the available data (Fig. 6A). Four nodes are strictly found in LE19-388.1, and six nodes are found in both LE19\_98.1 and LE19-13.4, highlighting chemical diversity of the metabolite class between strains.

BGC0001018.1: Microcystis aeruginosa K-139 mcnF, mcnA, mcnB, mcnC, mcnE, orf1, orf2, orf3 genes, complete cds

Cluster 15: appears in LE19-98.1

Cluster 4: appears in LE19-13.4 Cluster 8: appear in LE19-388.

## Putatively linking BGCs to spectra

To link candidate products and GCFs observed in the WLECC and putatively identify relationships between uncharacterized spectra and BGCs, *in silico* scoring approaches were used. For proof of concept, we assessed links between spectral data and the gene clusters putatively encoding anabaenopeptin (*apn*) and the PmNT3 cluster. NPlinker putatively linked six spectra to the *apn* gene cluster, including two annotated as anabaenopeptin NZ857 from the GNPS library database. In total, three features were identified as anabaenopeptins (two through GNPS, one through Sirius/ClassyFire), while an additional two features were coarsely identified as "Cyclic Peptides" using the Sirius workflow (Fig. 7A). These spectra may represent previously undescribed congeners of anabaenopeptin or structurally similar molecules outside of the anabaenopeptin class. Additionally linked candidate spectra received various generic annotations from Sirius/ClassyFire with variable confidence and may represent derivatives or intermediate synthesis products of anabaenopeptin, or false positives (Fig. 7A; Table S4). Detailed

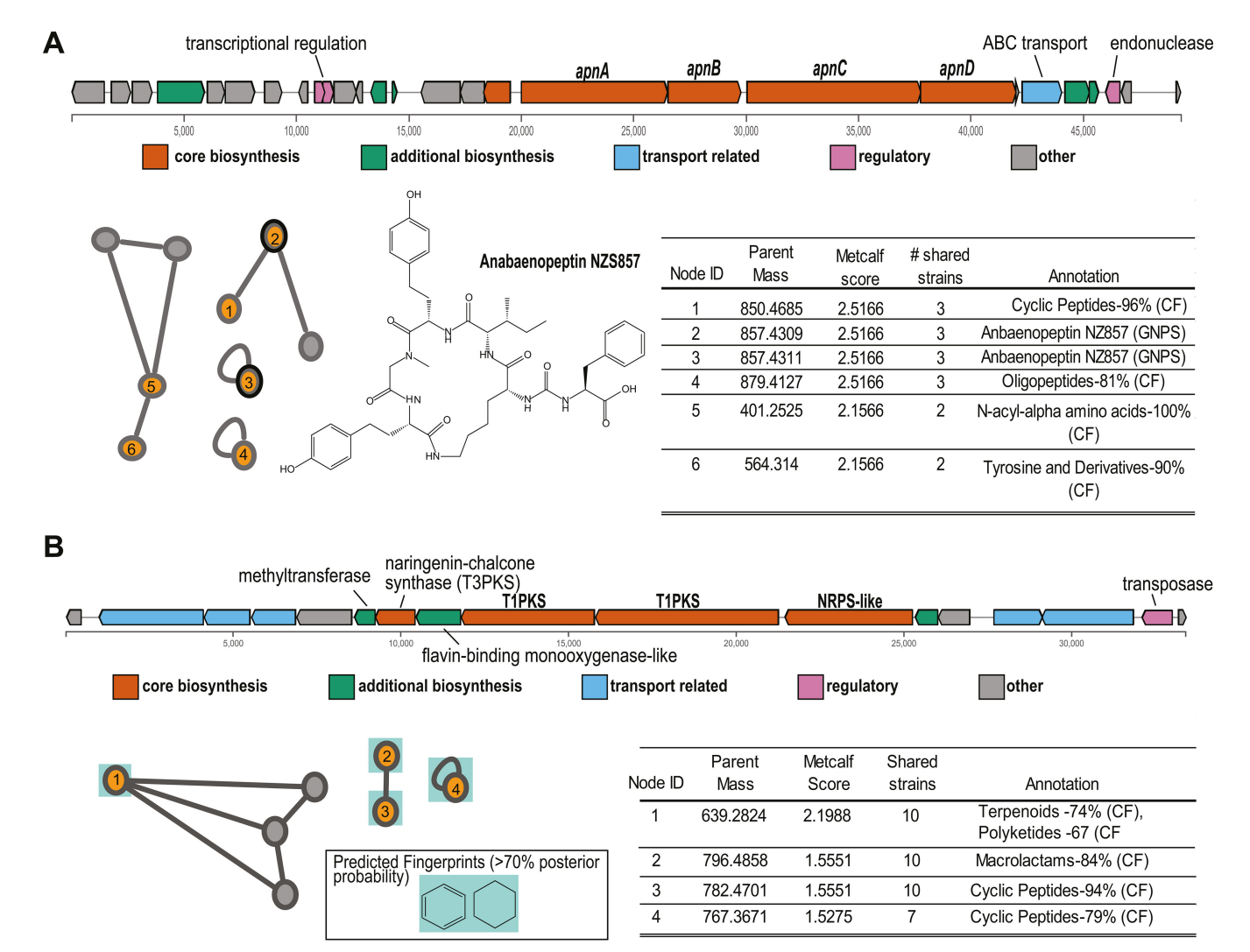


FIG 7 Spectra linked to the anabaenopeptin (A) *apn* and (B) PmNT3 gene clusters through NPLinker. Linked spectral features identified by NPlinker are colored orange, and the parent mass, Metcalf score, number of shared strains, and putative annotation via GNPS and/or ClassyFire are reported in the table. Gray nodes represent features that were not linked with NPlinker but were within subnetworks for putatively linked features. For the PmNT3 cluster, select molecular fingerprints including ring systems, halogenations, or sulfurous qualities are highlighted with differing colors.

annotations, select molecular fingerprints, and structure predictions for putatively linked spectra are shown in Table S4.

For the cryptic PmNT3 GCF, NPlinker identified four features that potentially represent biosynthesis products. Based on the highest Metcalf score, the best match was annotated as a molecule with terpenoid/polyketide-like qualities (74%/67% confidence) using Sirius/ClassyFire (64, 65). Additionally linked candidate spectra were also annotated generically with variable confidence (Fig. 7B). While it is unlikely that these chemical features are 100% matches to predicted annotations, their structural properties share some similarities with intermediate and completely biosynthesized [7,7] paracyclophane-like molecules. Molecular fingerprint annotations provide evidence that putatively linked spectra to the PmNT3 gene cluster consist of at least one ring system, a key feature in paracyclophanes (48, 49, 52). Detailed annotations, select molecular fingerprints, and structure predictions for putatively linked spectra are shown in Table S5. While we are unable to resolve the complete structure of the biosynthesis product from PmNT3, and putatively linked spectra may represent false positives, these results suggest that biosynthesis products from this GCF may contain chemical properties of paracyclophane molecules (66). Complete NPlinker results, which putatively link all identified GCFs and associated chemical features, can be found at https://github.com/ ceyancey/Metabalo-genomics-of-WLECC.

## **DISCUSSION**

We investigated *Microcystis* secondary metabolism through integrated analysis of BGCs and MS features of metabolites in cultures isolated from WLE. The cultures used in this study are not axenic, as they contain several bacteria known to associate with *Microcystis* in natural cyanoHAB communities (40, 67). Regardless, these cultures are simplified compared to environmental samples and thus valuable for laboratory study. While most WLECC cultures were isolated in 2017–2019 during early-to-peak phases of the bloom (40), they captured the genetic diversity of putative BGCs observed in the 2014 WLE cyanoHAB, as well as clusters not observed during that time (Fig. 1 and 2). By pairing metabolomics with genomic analyses, we identified known and novel secondary metabolites and putatively linked GCFs with chemical features through *in silico* approaches. Our study highlights several known BGCs, predicted biosynthesis products, and several uncharacterized clusters and features, revealing the vast breadth and diversity observed in *Microcystis* gene clusters and metabolomes that have yet to be described.

Both genomic and metabolomic analyses reveal the potential for several Microcystis strains to produce secondary metabolites with toxic properties, including microcystins, aeruginosins, cyanopeptolin/micropeptins, anabaenopeptins, and microginins (Fig. 1, 2, 4, and 6) (31, 33, 45, 68, 69). These results are consistent with the co-occurrence of secondary metabolites from Microcystis-dominated cyanoHABs in lakes and raw drinking waters (27, 28, 70). Growing evidence indicates that such combinations of multiple secondary metabolites can have compounding effects regarding bioactivity and/or toxicity (29). Our culture collection of Microcystis strains that contain variable suites of cyanopeptides within each culture (Fig. 4 and 5; Table S3) will be valuable in studying potential toxic and bioactive synergisms in mixtures of secondary metabolites. However, our results also emphasize that culture metabolomes provide a snapshot in time, and BGC presence is not indicative of a biosynthesis product, as different clusters may be expressed under different conditions (Fig. 5). Our untargeted approach also revealed greater congener diversity of various metabolites compared to approaches that employed standards for detection (27, 28, 70), although confidence in congener identity is lower without the use of standards. The greatest chemical diversity was observed for putatively identified cyanopeptolin/micropeptin features that were largely predicted by SNAP-MS (Fig. 4 and 6; Table S2). Level 3 confidence is reported for one of these micropeptin analogs due to further manual annotation (m/z 846.47), but we were not able to solve the structure of other micropeptins without further data collection or use

of standards (61). Cyanopeptolins, which are found globally (20), inhibit serine proteases and chymotrypsin, which can have neurotoxic effects (3, 71, 72) and disrupt food webs (73, 74).

In addition to identifying biosynthesis pathways and chemical features from known *Microcystis* secondary metabolites, our approach enabled the exploration of novel BGCs, including those putatively encoding biosynthesis of a [7,7] paracyclophane-like molecule. These metabolites contain structural symmetry and insertion of various functional groups and are believed to derive from decanoic acid (48, 49, 52, 75). To date, [7,7] paracyclophanes have only been isolated from fungal (76) or cyanobacterial sources, but a biosynthesis product has yet to be identified from *Microcystis*. Previous work has identified the presence of the PmNT3 cluster in several *Microcystis* genomes (75). This BGC also has an inverse relationship in transcriptional activity with the *mcy* operon (77), suggesting that produced metabolites may have tradeoffs or serve similar functions under different environmental conditions. Based on the reported cytotoxicity of other [7,7] paracyclophanes (52) and high transcriptional activity in the 2014 western Lake Erie cyanoHAB (26), its biosynthetic routes, chemical structure, and functional role are a high priority for continued research.

The *Microcystis* PmNT3 cluster lacks homologs to *cylC* and *cylK* (78), which are essential for the formation of the final macrocycle, suggesting that a linear analog may be biosynthesized (53, 75). However, our results also show the presence of a putative flavin-dependent monooxygenase-like gene within the BGC (PmNT3 8; Fig. 3; Table 1) that may catalyze macrocycle formation through C-H functionalization (53). Additionally, *cylC* homologs have previously been identified in *Microcystis* genomes (53), and we identified a putative *cylC* homolog in 9 out of 15 isolates that contain the putative cyclophane-encoding BGC (Table S6), though they were not co-localized with the PmNT3 cluster. Homologs for *cylK* were not detected in any of the *Microcystis* genomes. Missing *cylC* and *cylK* homologs likely reflects true gene absence as paired-end read mapping failed to detect these genes (data not shown). Together, the presence of a putative flavin-dependent monooxygenase-like gene within the PmNT3 cluster, as well as the presence *cylC* homologs within *Microcystis* isolates, suggests the possibility of a novel mode of [7,7] paracyclophane biosynthesis, but more research is needed to ascertain chemical structure and the complete biosynthetic pathway.

In silico approaches yielded a concise list of candidate spectra linked to GCFs of interest. By linking the apn GCF and chemical features annotated as anabaenopeptins, we provide proof-of-concept for the utility of in silico linking between genomic and metabolomic data (Fig. 7A). We also made conservative inferences regarding the uncharacterized gene cluster PmNT3 and unknown metabolites. While these inferences provide valuable hypotheses, given the low confidence in structure prediction by Sirius (Fig. 7B; Table S5) and the potential for false positives from NPlinker (62, 79), these hypotheses should be tested with further studies. For example, chemical fingerprints provide evidence that putative products of the PmNT3 cluster contain characteristic functional groups of paracyclophanes such as ring systems, but overall structure predictions do not provide high confidence in the detection of a paracyclophane molecule (Fig. 7B). Genetic annotation of the PmNT3 cluster provides evidence that a synthesis product would have greater polyketide character than peptidic character (Fig. 3; Table 1), while some lower scoring, putatively linked spectra are peptidic in nature (Fig. 7B). Because of this, some links may represent false positives and highlight the need for traditional structural elucidation approaches. While applications such as nuclear magnetic resonance (NMR) and heterologous expression to determine exact biosynthetic mechanisms and produced products are beyond the scope of this study, the PmNT3 case study highlights the need for future molecular approaches to determine the structure of the final-produced metabolite. The WLECC is an excellent resource for elucidating the chemical structure of secondary metabolites such as those encoded in the PmNT3 cluster, which was heretofore considered "orphan" (23, 26, 75).

Our results demonstrate the diversity and wealth of uncharacterized *Microcystis* biosynthesis pathways and metabolomes. While this study highlights a few BGCs, substantial biosynthetic potential can be explored through the WLECC, as evidenced by the abundance of unknown and coarsely annotated gene clusters and chemical features. Each culture appears to have a distinct metabolome (Fig. 4 and 5; Table S2) despite the similar BGC compositions observed between closely related or identical strains (Fig. 1). Identifying drivers of differential metabolome compositions is beyond the scope of this study but may be a result of different associated bacterial assemblages within cultures and microbial exchange of various substrates (40, 80, 81), or subtle differences in genomic sequences, which may encode slightly variable enzyme complexes leading to expanded structural diversity (82). Ultimately, these results may be used to better understand observed cyanoHAB dynamics in WLE and inform monitoring and management strategies to mitigate the impacts of toxic secondary metabolite production.

#### **MATERIALS AND METHODS**

## Western Lake Erie culture collection and sequencing

Collection, isolation, cultivation, and DNA extraction of *Microcystis* WLECC isolates have been recently described (40). Briefly, the WLECC consists of 21 xenic *Microcystis* isolates. Cultures were maintained in BG-112N medium, at 22.9°C, with a 12/12 hour light/dark cycle with light of 40 µmol photon/m²/s. DNA was extracted approximately 7 days after initial passaging with the DNeasy Blood and Tissue Kit (Qiagen, Hilden, Germany) and QIAShredder adapter (Qiagen, Hilden Germany) according to this protocol: https://www.protocols.io/view/dna-extraction-from-filters-using-qiagen-dneasy-an-jx5cpq6. DNA concentration was determined using the QuantIT PicroGreen dsDNA Assay Kit (Fisher Scientific, Waltham, MA, USA). Extracted DNA was sequenced at the University of Michigan Advanced Genomics Core (Ann Arbor, MI, USA) using the NovaSeq S4 platform (Illumina, San Diego, CA, USA) with 300 cycles. Paired end sequences were run with the maximum library fragment (insert) size possible without compromising read quality.

#### **Bioinformatic analysis**

Raw sequence reads were quality checked and processed using bbduk, from the Joint Genome Institute (JGI)-supported suite of tools, bbtools (83), to remove adapters, trim reads for quality, and remove contamination using the UniVec reference collection (https://www.ncbi.nlm.nih.gov/tools/vecscreen/univec/). Duplicate reads were removed using dedupe as part of the bbtools version 38.84 package as well. Individual *de novo* assemblies were completed for each isolate using Megahit v.1.2.9 with the meta-sensitive parameter (84). Contiguous sequences of at least 1,000 base pairs in length were kept for downstream analysis including creating an Anvi'o v.7 (85) database for each isolate. Each database was manually refined into *Microcystis* and associated bacteria metagenome-assembled genomes (MAGs) for each culture (40).

Each *Microcystis* MAG was then run through AntiSMASH v.6.0.1 (86) with default parameters under relaxed settings. BGCs were further analyzed if they were at least 5.5 kb in length, and contained NRPS, PKS, multi (NRPS and PKS combinations), microviridin, cyanobactin, lanthipeptide, RiPP, or spliceotide annotation via antiSMASH. BGCs annotated as terpenes were excluded from further analysis. A deduplicated list of BGCs was subjected to deep annotation, including gene-by-gene annotation using PFAM, TIGRfam, and blastP (Table S1). GCF analysis was completed using BiG-SCAPE (87) with default parameters.

To determine which *Microcystis* genomes contained which BGCs and their degree of completion, a series of mapping approaches were used. This was done due to the quality of *Microcystis* MAGs, which are considered drafts genomes, with variable N50s due to low coverage obtained through sequencing (40). First, BGC sequences were aligned to

genomes using BLAST (88). Positive hits were considered if the following criteria were met: at least 95% identity, at least 80% alignment length, and e-value no greater than  $1 \times 10^{-5}$ . For further confirmation of BGC presence in a particular *Microcystis* genome, especially for ambiguous alignments that did not satisfy the above parameters, read mapping and visualization were also completed. Briefly, bbmap from the JGI-supported bbmap tools package (83) was used to map QC reads from each *Microcystis* isolate onto BGCs setting the minID to 0.95, the IDfilter to 0.8, and allowing ambiguous reads to multimap. Read mapping alignments were then visually inspected in Tablet (89) to determine the presence or absence of core biosynthetic genes for each cluster based on the evenness of coverage patterns (see Fig. S5 for an example). This ensured the detection of complete BGCs that assembled poorly such as the *mcy* and *mcn* operons in some *Microcystis* isolates.

## **Protein modeling**

A homology model for PmNT3 8 was generated using SWISS-MODEL (90) software with the AlphaFold structure AF-A0A552JBG4-F1 (99.3% sequence identity with PmNT3 8) as a starting model. The PmNT3 8 homology model was used to query the protein data bank for structural homologs using the DALI server (91). Superposition of the PmNT3 8 homology model with AncFMO5 and AetF was performed using LSQ superpose in Coot (92). The figures were generated using PyMOL (Schrödinger).

## Mass spectrometry sample preparation and data acquisition

The following steps were completed for mass spectrometry sample preparation and data acquisition. All 21 cultures were grown in 50 mL of BG11-2N medium for 2 weeks. Once sufficient biomass was achieved, cultures were filtered onto 47 mm GF/F filters (Whatman, Maidstone, UK). Filters were stored at  $-80^{\circ}$ C until further analysis. Extractions were performed using a 50:50 HPLC grade methanol/chloroform extraction protocol. Briefly, thawed GF/F filters were suspended in 50:50 methanol/chloroform solution and sonicated for 30 minutes. The extraction was then mixed gently for 4 hours at 30°C, filtered to remove solids, dried under nitrogen, and stored at  $-20^{\circ}$ C until further analysis.

Ultra-high-performance liquid chromatograms (UHPLC) were obtained on an Agilent liquid chromatography-mass spectrometry system made up of an Agilent 1290 Infinity II UHPLC coupled to an Agilent 6545 ESI-Q-TOF-MS in positive ionization mode. Aliquots (1 µL) of the WLECC Microcystis extracts (1 mg/mL in methanol) were analyzed on a Kinetex phenyl-hexyl (1.7  $\mu$ m, 2.1  $\times$  50 mm) column using the described parameters and method in references (93). Briefly, a 1-minute isocratic elution of 90% A (A = 100% H<sub>2</sub>O and 0.1% formic acid) followed by 6-minute linear gradient elution to 100% B (B = 95% acetonitrile, 5% H<sub>2</sub>O, and 0.1% formic acid) with a flow rate of 0.4 mL/min was used followed by isocratic elution with 100% B for 2 minutes. The electrospray ionization (ESI) system was calibrated such that the capillary temperature was set to 320°C, the source voltage was 3.5 kV, and the gas flow rates were 11 L/min. lons above intensity 1,000 were detected and counted at 6 scans/s with a maximum of nine selected precursors per cycle using ramped collision energy (93). Data-dependent analysis was performed. The acquired MS/MS data were converted from Agilent (Agilent, Santa Clara, CA, USA) vendor data files (.d) to mzXML file format using MSConvert software through the Proteowizard package (94).

## Analysis and annotation of MS/MS data

A suite of *in silico* tools was used to process and analyze the mass spectrometry data to identify and annotate "features," which are defined as an ion signal of a specific mass-to-charge ratio (*m/z*) detected at a specific time (retention time-RT) that has an accompanying MS/MS spectrum available (95). First, MZMine v2.53 (96) was utilized for feature extraction and alignment across all WLECC extract MS samples, with alignment based on unique features across different samples being linked to a specific RT and

m/z. In MZMine v2.53, initial mass detection and filtering parameters were set with the MS1 threshold being 1e03 and the MS2 threshold being 1e02. Chromatogram building utilized a minimum group size number of scans as 2, a group intensity threshold of 2e04, a minimum highest intensity of 5e03, and m/z tolerance of 10 ppm. Chromatogram deconvolution utilized a chromatographic threshold of 50%, a search minimum RT range of 0.20 minutes, a minimum relative height of 10%, a minimum absolute height of 5e0, and a peak duration range 0-3 minutes, an m/z range for MS2 scan pairing of 0.1 Da, an RT range for MS2 scan pairing of 0.2 minutes, and a local minimum search algorithm. For isotope grouping, a m/z tolerance of 10 minutes, RT tolerance of 0.05 minutes, and a maximum charge of 2 were used. Alignment was conducted with a weight of 75 for m/z ratio and 25 for RT and an RT tolerance of 0.05. Downstream filtering in MZMine took place and is described below. In total, 2,784 features were extracted from positive and negative ionization mode MS/MS data and annotated with unique identification numbers. Associated feature intensities in each sample were identified based on peak areas in extracted-ion chromatograms. Features corresponding to extraction solvent and uninoculated growth medium were removed from the feature set, resulting in 1,307 total features in positive ionization mode for analysis.

Feature-based molecular networking (FBMN) through the GNPS (55, 95) was used to identify subnetworks of structurally related features. Connections (edges) and features (nodes) within the subnetworks can be visualized with Cytoscape software (97). Additionally, GNPS identifies spectral matches (exact or analogous metabolites) in submitted MS/MS data by searching through publicly available databases of MS/MS data, which were annotated in the Cytoscape molecular network. DER-EPLICATOR, built into the GNPS platform, was used for additional annotation of the molecular network in order to predict peptidic secondary metabolites with a P-value 5  $\times$  10<sup>-12</sup> or lower (57). Results for GNPS analysis (both positive and negative ionization mode) can be found at https://gnps.ucsd.edu/ProteoSAFe/status.jsp? task=64896147136e41ffaf17176f3d90937e and https://gnps.ucsd.edu/ProteoSAFe/status.jsp?task=36964d2641364f658e30f32629e85081, respectively. Lastly, annotations from SNAP-MS were used to assign compound families to subnetworks in the molecular network using groupings in the Natural Products Atlas (58, 98, 99). Final data outputs were visualized in Cytoscape v 3.9.1 (97). Annotations with spectral matches to databases in GNPS were given a level 3 annotation, and those annotations which had manual inspection and verification from this set were labeled as level 2 confidence, according to Schymanski principles (61). Annotations made by DEREPLICATOR and SNAP-MS were annotated as level 5. Manual annotations of the cyanopeptides were conducted using library reference mirror plots from GNPS (Fig. S5) and manual annotations of mass changes corresponding to amino acids and other fragments of the molecule (Micropeptin MZ 845). CyanometDB was utilized to verify the MS1 and molecular formula of the manually annotated metabolites (56).

# In silico putative linking of GCFs and spectral data

The software NPlinker was used to putatively link BGCs with spectral data (62). NPlinker requires outputs from BIG-Scape, AntiSMASH, and GNPS to putatively link candidate synthesis products and GCFs. The NPlinker analysis was run on Docker according to the workflow described at <a href="https://github.com/NPLinker/nplinker-webapp">https://github.com/NPLinker/nplinker-webapp</a>. We report putative links between GCFs and spectral data, along with the parent mass, number of shared strains, and Metcalf scores for *apn* and PmNT3 clusters. Putatively linked spectra to GCFs of interest were additionally annotated using the SIRIUS workflow (65, 100, 101).

## Statistical analysis and figure rendering

Figures were generated in R on R Studio (102) using the packages ggplot2 (103) and ggpubr (104). GCF networks and BGC gene schematics were generated in BiG-SCAPE (87) and edited further for visual clarity in Cytoscape (97). Metabolomic networks were generated by GNPS and further refined in Cytoscape as well.

#### **ACKNOWLEDGMENTS**

We thank Robert Hein and Teal Furnholm for the bioinformatic support. We also thank all members of the Geomicrobiology Lab for their help in cultivating and maintaining the WLECC.

This work was supported by NIH and NSF awards to the Great Lakes Center for Fresh Waters and Human Health (NIH: 1P01ES028939-01 and NSF: OCE-1840715), the Cooperative Institute of Great Lakes Research (NA17OAR4320152), and the Hans W. Vahlteich Professorship. Support was also provided by UM Natural Products Biosciences Initiative, NOAA OAR 'Omics, and NOAA OAR Ocean Technology Development Initiative.

#### **AUTHOR AFFILIATIONS**

<sup>1</sup>Department of Earth and Environmental Sciences, University of Michigan, Ann Arbor, Michigan, USA

<sup>2</sup>Program in Chemical Biology, University of Michigan, Ann Arbor, Michigan, USA

<sup>3</sup>Life Sciences Institute, University of Michigan, Ann Arbor, Michigan, USA

<sup>4</sup>Departments of Medicinal Chemistry, Chemistry, Microbiology, and Immunology, University of Michigan, Ann Arbor, Michigan, USA

<sup>5</sup>Natural Products Discovery Core, Life Sciences Institute, University of Michigan, Ann Arbor, Michigan, USA

<sup>6</sup>Pharmacognosy Department, Faculty of Pharmacy, Cairo University, Cairo, Egypt

<sup>7</sup>Cooperative Institute for Great Lakes Research (CIGLR), School for Environment and Sustainability, University of Michigan, Ann Arbor, Michigan, USA

## **AUTHOR ORCIDs**

Colleen E. Yancey http://orcid.org/0000-0002-6078-9483
Lauren Hart http://orcid.org/0000-0001-8553-2839
David H. Sherman http://orcid.org/0000-0001-8334-3647
Gregory J. Dick http://orcid.org/0000-0001-7666-6288

#### **FUNDING**

Funder	Grant(s)	Author(s)
HHS   NIH   National Institute of Environmental Health Sciences (NIEHS)	1P01ES028939-01	Gregory J. Dick
National Science Foundation (NSF)	OCE-1840715	Gregory J. Dick
Cooperative Institute for Great Lakes Research (CIGLR)	NA17OAR4320152	Gregory J. Dick
Hans W. Vahltiech Professorship		David H. Sherman
UM Natural Products Biosciences Initiative		Ashootosh Tripathi
NOAA OAR 'Omics and Ocean Technology Development Initiative		Gregory J. Dick

## **DATA AVAILABILITY**

Raw reads and metagenome assembled genomes (MAGs) were deposited at the respective NCBI repositories and are available in BioProject PRJNA903891. Raw reads are available under the SRA accession numbers: SRR22360640–SRR22360660. Raw mxXML files for metabolomic data can be found at https://massive.ucsd.edu/ProteoSAFe/dataset.jsp?task=cd03648b2a174e4697c123db59db40bf.

# **ADDITIONAL FILES**

The following material is available online.

#### Supplemental Material

**Supplemental Figures (mSystems00334-24-s0001.docx).** Supplemental table captions and Figures S1 to S6.

Supplemental Tables (mSystems00334-24-s0002.xlsx). Tables 1–6.

#### REFERENCES

- Harke MJ, Steffen MM, Gobler CJ, Otten TG, Wilhelm SW, Wood SA, Paerl HW. 2016. A review of the global ecology, genomics, and biogeography of the toxic cyanobacterium. Harmful Algae 54:4–20. https://doi.org/10. 1016/j.hal.2015.12.007
- Huisman J, Codd GA, Paerl HW, Ibelings BW, Verspagen JMH, Visser PM.
   2018. Cyanobacterial blooms. Nat Rev Microbiol 16:471–483. https://doi.org/10.1038/s41579-018-0040-1
- Welker M, von Döhren H. 2006. Cyanobacterial peptides nature's own combinatorial biosynthesis. FEMS Microbiol Rev 30:530–563. https:// doi.org/10.1111/j.1574-6976.2006.00022.x
- Kehr J-C, Gatte Picchi D, Dittmann E. 2011. Natural product biosyntheses in cyanobacteria: A treasure trove of unique enzymes. Beilstein J Org Chem 7:1622–1635. https://doi.org/10.3762/bjoc.7.191
- Dittmann E, Gugger M, Sivonen K, Fewer DP. 2015. Natural product biosynthetic diversity and comparative genomics of the cyanobacteria. Trends Microbiol. 23:642–652. https://doi.org/10.1016/j.tim.2015.07.008
- Liu J, Van Oosterhout E, Faassen EJ, Lürling M, Helmsing NR, Van de Waal DB. 2016. Elevated pCO2 causes a shift towards more toxic microcystin variants in nitrogen-limited *Microcystis aeruginosa*. FEMS Microbiol Ecol 92:1–8. https://doi.org/10.1093/femsec/fiv159
- Chapra SC, Boehlert B, Fant C, Bierman VJ, Henderson J, Mills D, Mas DML, Rennels L, Jantarasami L, Martinich J, Strzepek KM, Paerl HW. 2017. Climate change impacts on harmful Algal blooms in U.S. freshwaters: a screening-level assessment. Environ Sci Technol 51:8933– 8943. https://doi.org/10.1021/acs.est.7b01498
- Griffith AW, Gobler CJ. 2020. Harmful algal blooms: a climate change co-stressor in marine and freshwater ecosystems. Harmful Algae 91:101590. https://doi.org/10.1016/j.hal.2019.03.008
- Davis TW, Berry DL, Boyer GL, Gobler CJ. 2009. The effects of temperature and nutrients on the growth and dynamics of toxic and non-toxic strains of *Microcystis* during cyanobacteria blooms. Harmful Algae 8:715–725. https://doi.org/10.1016/j.hal.2009.02.004
- Hellweger FL, Martin RM, Eigemann F, Smith DJ, Dick GJ, Wilhelm SW. 2022. Models predict planned phosphorus load reduction will make Lake Erie more toxic. Science 376:1001–1005. https://doi.org/10.1126/ science.abm6791
- Wagner ND, Osburn FS, Wang J, Taylor RB, Boedecker AR, Chambliss CK, Brooks BW, Scott JT. 2019. Biological stoichiometry regulates toxin production in *Microcystis aeruginosa* (UTEX 2385). Toxins (Basel) 11:601. https://doi.org/10.3390/toxins11100601
- Botes DP, Tuinman AA, Wessels PL, Viljoen CC, Kruger H, Williams DH, Santikarn S, Smith RJ, Hammond SJ. 1984. The structure of cyanoginosin-LA, a cyclic heptapeptide toxin from the cyanobacterium *Microcystis* aeruginosa. J Chem Soc Perkin Trans 1:2311. https://doi.org/10.1039/ p19840002311
- Carmichael WW. 1992. Cyanobacteria secondary metabolites-the cyanotoxins. J Appl Bacteriol 72:445–459. https://doi.org/10.1111/j. 1365-2672.1992.tb01858.x
- Qin B, Zhu G, Gao G, Zhang Y, Li W, Paerl HW, Carmichael WW. 2010. A drinking water crisis in Lake Taihu, China: linkage to climatic variability and lake management. Environ Manage 45:105–112. https://doi.org/10. 1007/s00267-009-9393-6
- Steffen MM, Davis TW, McKay RML, Bullerjahn GS, Krausfeldt LE, Stough JMA, Neitzey ML, Gilbert NE, Boyer GL, Johengen TH, Gossiaux DC, Burtner AM, Palladino D, Rowe MD, Dick GJ, Meyer KA, Levy S, Boone BE, Stumpf RP, Wynne TT, Zimba PV, Gutierrez D, Wilhelm SW. 2017. Ecophysiological examination of the Lake Erie Microcystis bloom in 2014: linkages between biology and the water supply shutdown of Toledo, OH. Environ Sci Technol 51:6745–6755. https://doi.org/10.1021/ acs.est.7b00856
- Roegner A, Sitoki L, Weirich C, Corman J, Owage D, Umami M, Odada E, Miruka J, Ogari Z, Smith W, Rejmankova E, Miller TR. 2020. Harmful algal

- blooms threaten the health of peri-urban fisher communities: a case study in Kisumu Bay, Lake Victoria, Kenya. Expo Health 12:835–848. https://doi.org/10.1007/s12403-019-00342-8
- Stewart I, Seawright AA, Shaw GR. 2008. Cyanobacterial poisoning in livestock, wild mammals and birds—an overview. Adv Exp Med Biol 619:613–637. https://doi.org/10.1007/978-0-387-75865-7\_28
- Jochimsen EM, Carmichael WW, An JS, Cardo DM, Cookson ST, Holmes CE, Antunes MB, de Melo Filho DA, Lyra TM, Barreto VS, Azevedo SM, Jarvis WR. 1998. Liver failure and death after exposure to microcystins at a hemodialysis center in Brazil. N Engl J Med 338:873–878. https:// doi.org/10.1056/NEJM199803263381304
- Pouria S, de Andrade A, Barbosa J, Cavalcanti RL, Barreto VT, Ward CJ, Preiser W, Poon GK, Neild GH, Codd GA. 1998. Fatal microcystin intoxication in Haemodialysis unit in Caruaru, Brazil. Lancet 352:21–26. https://doi.org/10.1016/s0140-6736(97)12285-1
- Janssen EML. 2019. Cyanobacterial peptides beyond microcystins a review on co-occurrence, toxicity, and challenges for risk assessment. Water Res 151:488–499. https://doi.org/10.1016/j.watres.2018.12.048
- Breinlinger S, Phillips TJ, Haram BN, Mareš J, Martínez Yerena JA, Hrouzek P, Sobotka R, Henderson WM, Schmieder P, Williams SM, Lauderdale JD, Wilde HD, Gerrin W, Kust A, Washington JW, Wagner C, Geier B, Liebeke M, Enke H, Niedermeyer THJ, Wilde SB. 2021. Hunting the eagle killer: a cyanobacterial neurotoxin causes vacuolar myelinopathy. Science 371:eaax9050. https://doi.org/10.1126/science. aax9050
- Lima ST, Fallon TR, Cordoza JL, Chekan JR, Delbaje E, Hopiavuori AR, Alvarenga DO, Wood SM, Luhavaya H, Baumgartner JT, Dörr FA, Etchegaray A, Pinto E, McKinnie SMK, Fiore MF, Moore BS. 2022. Biosynthesis of guanitoxin enables global environmental detection in freshwater cyanobacteria. J Am Chem Soc 144:9372–9379. https://doi. org/10.1021/jacs.2c01424
- Humbert J-F, Barbe V, Latifi A, Gugger M, Calteau A, Coursin T, Lajus A, Castelli V, Oztas S, Samson G, Longin C, Medigue C, de Marsac NT. 2013. A tribute to disorder in the genome of the bloom-forming freshwater cyanobacterium *Microcystis aeruginosa*. PLoS One 8:e70747. https://doi. org/10.1371/journal.pone.0070747
- Dick GJ, Duhaime MB, Evans JT, Errera RM, Godwin CM, Kharbush JJ, Nitschky HS, Powers MA, Vanderploeg HA, Schmidt KC, Smith DJ, Yancey CE, Zwiers CC, Denef VJ. 2021. The genetic and Ecophysiological diversity of *Microcystis*. Environ Microbiol 23:7278–7313. https://doi. org/10.1111/1462-2920.15615
- Pérez-Carrascal OM, Terrat Y, Giani A, Fortin N, Greer CW, Tromas N, Shapiro BJ. 2019. Coherence of Microcystis species revealed through population genomics. ISME J 13:2887–2900. https://doi.org/10.1038/ s41396-019-0481-1
- Yancey CE, Yu F, Tripathi A, Sherman DH, Dick GJ. 2022. Expression of Microcystis biosynthetic gene clusters in natural populations suggests temporally dynamic synthesis of novel and known secondary metabolites in Western Lake Erie. Microbiology. https://doi.org/10. 1101/2022.10.12.511943
- Beversdorf LJ, Rude K, Weirich CA, Bartlett SL, Seaman M, Kozik C, Biese P, Gosz T, Suha M, Stempa C, Shaw C, Hedman C, Piatt JJ, Miller TR. 2018. Analysis of cyanobacterial metabolites in surface and raw drinking waters reveals more than microcystin. Water Res. 140:280–290. https://doi.org/10.1016/j.watres.2018.04.032
- Beversdorf LJ, Weirich CA, Bartlett SL, Miller TR. 2017. Variable cyanobacterial toxin and metabolite profiles across six eutrophic lakes of differing physiochemical characteristics. Toxins 9:62. https://doi.org/ 10.3390/toxins9020062
- Pawlik-Skowrońska B, Bownik A. 2022. Synergistic toxicity of some cyanobacterial oligopeptides to physiological activities of *Daphnia*

10.1128/msystems.00334-24**17** 

- magna (Crustacea). Toxicon 206:74–84. https://doi.org/10.1016/j.toxicon.2021.12.013
- Martin C, Oberer L, Ino T, König WA, Busch M, Weckesser J. 1993.
   Cyanopeptolins, new depsipeptides from the cyanobacterium Microcystis sp. pcc 7806. J Antibiot. 46:1550–1556. https://doi.org/10. 7164/antibiotics.46.1550
- Ersmark K, Del Valle JR, Hanessian S. 2008. Chemistry and biology of the aeruginosin family of serine protease inhibitors. Angew Chem Int Ed 47:1202–1223. https://doi.org/10.1002/anie.200605219
- Martins J, Vasconcelos V. 2015. Cyanobactins from cyanobacteria: current genetic and chemical state of knowledge. Mar Drugs 13:6910–6946. https://doi.org/10.3390/md13116910
- Ishida K, Matsuda H, Murakami M. 1998. Four new microginins, linear peptides from the cyanobacterium *Microcystis aeruginosa*. Tetrahedron 54:13475–13484. https://doi.org/10.1016/S0040-4020(98)00826-6
- Ishida K, Nakagawa H, Murakami M. 2000. Microcyclamide, a cytotoxic cyclic hexapeptide from the cyanobacterium *Microcystis aeruginosa*. J Nat Prod 63:1315–1317. https://doi.org/10.1021/np000159p
- Bouaïcha N, Miles CO, Beach DG, Labidi Z, Djabri A, Benayache NY, Nguyen-Quang T. 2019. Structural diversity, characterization and toxicology of microcystins. Toxins (Basel) 11:714. https://doi.org/10. 3390/toxins11120714
- Allinger LE, Reavie ED. 2013. The ecological history of Lake Erie as recorded by the phytoplankton community. J Great Lakes Res 39:365– 382. https://doi.org/10.1016/j.jglr.2013.06.014
- Bridgeman TB, Chaffin JD, Filbrun JE. 2013. A novel method for tracking Western Lake Erie *Microcystis* blooms, 2002–2011. J Great Lakes Res 39:83–89. https://doi.org/10.1016/j.jglr.2012.11.004
- Watson SB, Miller C, Arhonditsis G, Boyer GL, Carmichael W, Charlton MN, Confesor R, Depew DC, Höök TO, Ludsin SA, Matisoff G, McElmurry SP, Murray MW, Peter Richards R, Rao YR, Steffen MM, Wilhelm SW. 2016. The re-eutrophication of Lake Erie: harmful algal blooms and hypoxia. Harmful Algae 56:44–66. https://doi.org/10.1016/j.hal.2016.04. 010
- Kasich J, Taylor M, Butler C, Zehringer J, Hodges R. 2015. State of Ohio harmful algal bloom response strategy for recreational waters. Technical Report. Obio Environmental Protection Agency.
- Yancey CE, Kiledal EA, Denef VJ, Errera RM, Evans JT, Hart L, Isailovic D, James W, Kharbush JK, Kimbrel JA, Li W, Mayali X, Nitschky H, Polik C, Powers MA, Premathilaka SH, Rappuhn N, Reitz LA, Rivera SR, Zwiers CC, Dick GJ. 2022. The Western Lake Erie culture collection: a promising resource for evaluating the physiological and genetic diversity of *Microcystis* and its associated microbiome. Microbiology. https://doi. org/10.1101/2022.10.21.513177
- Brittain SM, Wang J, Babcock-Jackson L, Carmichael WW, Rinehart KL, Culver DA. 2000. Isolation and characterization of *Microcystins*, cyclic heptapeptide hepatotoxins from a Lake Erie strain of *Microcystis* aeruginosa. J Great Lakes Res 26:241–249. https://doi.org/10.1016/ S0380-1330(00)70690-3
- Yancey CE, Smith DJ, Den Uyl PA, Mohamed OG, Yu F, Ruberg SA, Chaffin JD, Goodwin KD, Tripathi A, Sherman DH, Dick GJ. 2022. Metagenomic and metatranscriptomic insights into population diversity of microcystis blooms: spatial and temporal dynamics of mcy genotypes, including a partial operon that can be abundant and expressed. Appl Environ Microbiol 88:e0246421. https://doi.org/10. 1128/aem.02464-21
- 43. Yancey CE, Kiledal EA, Chaganti SR, Denef VJ, Errera RM, Evans JT, Hart LN, Isailovic D, James WS, Kharbush JJ, Kimbrel JA, Li W, Mayali X, Nitschky H, Polik CA, Powers MA, Premathilaka SH, Rappuhn NA, Reitz LA, Rivera SR, Zwiers CC, Dick GJ. 2023. The Western Lake Erie culture collection: a promising resource for evaluating the physiological and genetic diversity of Microcystis and its associated microbiome. Harmful Algae 126:102440. https://doi.org/10.1016/j.hal.2023.102440
- 44. Medema MH, Kottmann R, Yilmaz P, Cummings M, Biggins JB, Blin K, de Bruijn I, Chooi YH, Claesen J, Coates RC, et al. 2015. Minimum information about a biosynthetic gene cluster. Nat Chem Biol 11:625–631. https://doi.org/10.1038/nchembio.1890
- Bister B, Keller S, Baumann HI, Nicholson G, Weist S, Jung G, Süssmuth RD, Jüttner F. 2004. Cyanopeptolin 963A, a chymotrypsin inhibitor of Microcystis PCC 7806. J Nat Prod 67:1755–1757. https://doi.org/10. 1021/np049828f

- Tonk L, Welker M, Huisman J, Visser PM. 2009. Production of cyanopeptolins, anabaenopeptins, and microcystins by the harmful cyanobacteria *Anabaena* 90 and *Microcystis* PCC 7806. Harmful Algae 8:219–224. https://doi.org/10.1016/j.hal.2008.05.005
- Ziemert N, Ishida K, Liaimer A, Hertweck C, Dittmann E. 2008. Ribosomal synthesis of tricyclic depsipeptides in bloom-forming cyanobacteria. Angew Chem Int Ed Engl 47:7756–7759. https://doi.org/ 10.1002/anie.200802730
- May DS, Chen W-L, Lantvit DD, Zhang X, Krunic A, Burdette JE, Eustaquio A, Orjala J. 2017. Merocyclophanes C and D from the cultured freshwater cyanobacterium *Nostoc* sp. J Nat Prod 80:1073– 1080. https://doi.org/10.1021/acs.jnatprod.6b01175
- Nakamura H, Hamer HA, Sirasani G, Balskus EP. 2012. Cylindrocyclophane biosynthesis involves functionalization of an unactivated carbon center. J Am Chem Soc. 134:18518–18521. https://doi.org/10.1021/ ja308318p
- 50. Preisitsch M, Heiden SE, Beerbaum M, Niedermeyer THJ, Schneefeld M, Herrmann J, Kumpfmüller J, Thürmer A, Neidhardt I, Wiesner C, Daniel R, Müller R, Bange F-C, Schmieder P, Schweder T, Mundt S. 2016. Effects of halide lons on the carbamidocyclophane biosynthesis in nostoc sp. CAVN2. Marine Drugs 14:21. https://doi.org/10.3390/md14010021
- Moore BS, Chen JL, Patterson GML, Moore RE, Brinen LS, Kato Y, Clardy J. 1990. [7.7]Paracyclophanes from blue-green algae. J Am Chem Soc 112:4061–4063. https://doi.org/10.1021/ja00166a066
- Bui HTN, Jansen R, Pham HTL, Mundt S. 2007. Carbamidocyclophanes A–E, chlorinated paracyclophanes with cytotoxic and antibiotic activity from the vietnamese cyanobacterium *Nostoc* SP. J Nat Prod 70:499–503. https://doi.org/10.1021/np060324m
- Eusebio N, Rego A, Glasser NR, Castelo-Branco R, Balskus EP, Leão PN. 2021. Distribution and diversity of dimetal-carboxylate halogenases in cyanobacteria. BMC Genomics 22. https://doi.org/10.1186/s12864-021-07939-x
- Gäfe S, Niemann HH. 2023. Structural basis of regioselective tryptophan dibromination by the single-component flavin-dependent halogenase AetF. Acta Crystallogr D Struct Biol 79:596–609. https://doi.org/10.1107/ S2059798323004254
- Wang M, Carver JJ, Phelan VV, Sanchez LM, Garg N, Peng Y, Nguyen DD, Watrous J, Kapono CA, Luzzatto-Knaan T, et al. 2016. Sharing and community curation of mass spectrometry data with global natural products social molecular networking. Nat Biotechnol 34:828–837. https://doi.org/10.1038/nbt.3597
- Jones MR, Pinto E, Torres MA, Dörr F, Mazur-Marzec H, Szubert K, Tartaglione L, Dell'Aversano C, Miles CO, Beach DG, McCarron P, Sivonen K, Fewer DP, Jokela J, Janssen EM-L. 2021. CyanoMetDB, a comprehensive public database of secondary metabolites from cyanobacteria. Water Res. 196:117017. https://doi.org/10.1016/j.watres. 2021.117017
- 57. Mohimani H, Gurevich A, Mikheenko A, Garg N, Nothias L-F, Ninomiya A, Takada K, Dorrestein PC, Pevzner PA. 2017. Dereplication of peptidic natural products through database search of mass spectra. Nat Chem Biol 13:30–37. https://doi.org/10.1038/nchembio.2219
- Morehouse NJ, Clark TN, McMann EJ, van Santen JA, Haeckl FPJ, Gray CA, Linington RG. 2023. Annotation of natural product compound families using molecular networking topology and structural similarity fingerprinting. Nat Commun 14:308. https://doi.org/10.1038/s41467-022-35734-z
- Zervou SK, Gkelis S, Kaloudis T, Hiskia A, Mazur-Marzec H. 2020. New microginins from cyanobacteria of greek freshwaters. Chemosphere 248:125961. https://doi.org/10.1016/j.chemosphere.2020.125961
- Kang H-S, Krunic A, Shen Q, Swanson SM, Orjala J. 2011. Minutissamides A–D, antiproliferative cyclic decapeptides from the cultured cyanobacterium *Anabaena minutissima*. J Nat Prod 74:1597–1605. https://doi.org/10.1021/np2002226
- Schymanski EL, Jeon J, Gulde R, Fenner K, Ruff M, Singer HP, Hollender J. 2014. Identifying small molecules via high resolution mass spectrometry: communicating confidence. Environ Sci Technol 48:2097–2098. https://doi.org/10.1021/es5002105
- 62. Hjörleifsson Eldjárn G, Ramsay A, van der Hooft JJJ, Duncan KR, Soldatou S, Rousu J, Daly R, Wandy J, Rogers S. 2021. Ranking microbial metabolomic and genomic links in the NPLinker framework using

- complementary scoring functions. PLOS Comput Biol 17:e1008920. https://doi.org/10.1371/journal.pcbi.1008920
- Duncan KR, Crüsemann M, Lechner A, Sarkar A, Li J, Ziemert N, Wang M, Bandeira N, Moore BS, Dorrestein PC, Jensen PR. 2015. Molecular networking and pattern-based genome mining improves discovery of biosynthetic gene clusters and their products from salinispora species. Chem Biol 22:460–471. https://doi.org/10.1016/j.chembiol.2015.03.010
- Djoumbou Feunang Y, Eisner R, Knox C, Chepelev L, Hastings J, Owen G, Fahy E, Steinbeck C, Subramanian S, Bolton E, Greiner R, Wishart DS. 2016. ClassyFire: automated chemical classification with a comprehensive, computable taxonomy. J Cheminform 8:61. https://doi.org/10. 1186/s13321-016-0174-y
- Dührkop K, Fleischauer M, Ludwig M, Aksenov AA, Melnik AV, Meusel M, Dorrestein PC, Rousu J, Böcker S. 2019. SIRIUS 4: a rapid tool for turning tandem mass spectra into metabolite structure information. Nat Methods 16:299–302. https://doi.org/10.1038/s41592-019-0344-8
- Martins TP, Rouger C, Glasser NR, Freitas S, de Fraissinette NB, Balskus EP, Tasdemir D, Leão PN. 2019. Chemistry, bioactivity and biosynthesis of cyanobacterial alkylresorcinols. Nat Prod Rep 36:1437–1461. https:// doi.org/10.1039/c8np00080h
- Smith DJ, Tan JY, Powers MA, Lin XN, Davis TW, Dick GJ. 2021. Individual microcystis colonies harbour distinct bacterial communities that differ by microcystis oligotype and with time. Environ Microbiol 23:3020– 3036. https://doi.org/10.1111/1462-2920.15514
- Köcher S, Resch S, Kessenbrock T, Schrapp L, Ehrmann M, Kaiser M.
   2020. From dolastatin 13 to cyanopeptolins, micropeptins, and lyngbyastatins: the chemical biology of AHP-cyclodepsipeptides. Nat Prod Rep 37:163–174. https://doi.org/10.1039/C9NP00033J
- 69. Lenz KA, Miller TR, Ma H. 2019. Anabaenopeptins and cyanopeptolins induce systemic toxicity effects in a model organism the nematode *Caenorhabditis elegans*. Chemosphere 214:60–69. https://doi.org/10.1016/j.chemosphere.2018.09.076
- Kust A, Řeháková K, Vrba J, Maicher V, Mareš J, Hrouzek P, Chiriac M-C, Benedová Z, Tesařová B, Saurav K. 2020. Insight into unprecedented diversity of cyanopeptides in eutrophic ponds using an MS/MS networking approach. Toxins 12:561. https://doi.org/10.3390/ toxins12090561
- Faltermann S, Zucchi S, Kohler E, Blom JF, Pernthaler J, Fent K. 2014. Molecular effects of the cyanobacterial toxin cyanopeptolin (CP1020) occurring in algal blooms: global transcriptome analysis in zebrafish embryos. Aquatic Toxicology 149:33–39. https://doi.org/10.1016/j. aquatox.2014.01.018
- Gademann K, Portmann C, Blom JF, Zeder M, Jüttner F. 2010. Multiple toxin production in the cyanobacterium *Microcystis*: isolation of the toxic protease inhibitor cyanopeptolin 1020. J Nat Prod 73:980–984. https://doi.org/10.1021/np900818c
- Sadler T, von Elert E. 2014. Physiological interaction of *Daphnia* and Microcystis with regard to cyanobacterial secondary metabolites. Aquat Toxicol 156:96–105. https://doi.org/10.1016/j.aquatox.2014.08. 003
- 74. Pawlik-Skowrońska B, Toporowska M, Mazur-Marzec H. 2019. Effects of secondary metabolites produced by different cyanobacterial populations on the freshwater zooplankters *Brachionus calyciflorus* and *Daphnia pulex*. Environ Sci Pollut Res Int 26:11793–11804. https://doi.org/10.1007/s11356-019-04543-1
- Larsen JS, Pearson LA, Neilan BA. 2021. Genome mining and evolutionary analysis reveal diverse type III polyketide synthase pathways in cyanobacteria. Genome Biol Evol 13:evab056. https://doi.org/10.1093/ gbe/evab056
- Ohashi M, Kakule TB, Tang M-C, Jamieson CS, Liu M, Zhao Y-L, Houk KN, Tang Y. 2021. Biosynthesis of para-cyclophane-containing hirsutellone family of fungal natural products. J Am Chem Soc 143:5605–5609. https://doi.org/10.1021/jacs.1c00098
- Makower AK, Schuurmans JM, Groth D, Zilliges Y, Matthijs HCP, Dittmann E. 2015. Transcriptomics-aided dissection of the intracellular and extracellular roles of microcystin in *Microcystis aeruginosa* PCC 7806. Appl Environ Microbiol 81:544–554. https://doi.org/10.1128/AEM. 02601-14
- Braffman NR, Ruskoski TB, Davis KM, Glasser NR, Johnson C, Okafor CD,
   Boal AK, Balskus EP. 2022. Structural basis for an unprecedented

- enzymatic alkylation in cylindrocyclophane biosynthesis. Elife 11:e75761. https://doi.org/10.7554/eLife.75761
- Soldatou S, Eldjárn GH, Ramsay A, van der Hooft JJJ, Hughes AH, Rogers S, Duncan KR. 2021. Comparative metabologenomics analysis of polar actinomycetes. Mar Drugs 19:103. https://doi.org/10.3390/md19020103
- Baran R, Brodie EL, Mayberry-Lewis J, Hummel E, Da Rocha UN, Chakraborty R, Bowen BP, Karaoz U, Cadillo-Quiroz H, Garcia-Pichel F, Northen TR. 2015. Exometabolite niche partitioning among sympatric soil bacteria. Nat Commun 6:8289. https://doi.org/10.1038/ncomms9289
- 81. Phelan VV, Liu W-T, Pogliano K, Dorrestein PC. 2012. Microbial metabolic exchange—the chemotype-to-phenotype link. Nat Chem Biol 8:26–35. https://doi.org/10.1038/nchembio.739
- Gu L, Wang B, Kulkarni A, Geders TW, Grindberg RV, Gerwick L, Håkansson K, Wipf P, Smith JL, Gerwick WH, Sherman DH. 2009. Metamorphic enzyme assembly in polyketide diversification. Nature 459:731–735. https://doi.org/10.1038/nature07870
- 83. Bushnell B. BBTools user guide DOE joint genome institute. Available from: https://sourceforge.net/projects/bbmap. Retrieved 9 Apr 2021.
- Li D, Liu C-M, Luo R, Sadakane K, Lam T-W. 2015. MEGAHIT: an ultra-fast single-node solution for large and complex metagenomics assembly via succinct de bruijn graph. Bioinformatics 31:1674–1676. https://doi. org/10.1093/bioinformatics/btv033
- Eren AM, Kiefl E, Shaiber A, Veseli I, Miller SE, Schechter MS, Fink I, Pan JN, Yousef M, Fogarty EC, et al. 2021. Community-led, integrated, reproducible multi-omics with anvi'o. Nat Microbiol 6:3–6. https://doi. org/10.1038/s41564-020-00834-3
- Blin K, Shaw S, Kloosterman AM, Charlop-Powers Z, van Wezel GP, Medema MH, Weber T. 2021. antiSMASH 6.0: improving cluster detection and comparison capabilities. Nucleic Acids Res. 49:W29–W35. https://doi.org/10.1093/nar/gkab335
- 87. Navarro-Muñoz JC, Selem-Mojica N, Mullowney MW, Kautsar SA, Tryon JH, Parkinson EI, De Los Santos ELC, Yeong M, Cruz-Morales P, Abubucker S, Roeters A, Lokhorst W, Fernandez-Guerra A, Cappelini LTD, Goering AW, Thomson RJ, Metcalf WW, Kelleher NL, Barona-Gomez F, Medema MH. 2020. A computational framework to explore large-scale biosynthetic diversity. Nat Chem Biol 16:60–68. https://doi.org/10.1038/s41589-019-0400-9
- 88. Madden T. 2013. The BLAST sequence analysis tool.
- Milne I, Stephen G, Bayer M, Cock PJA, Pritchard L, Cardle L, Shaw PD, Marshall D. 2013. Using tablet for visual exploration of secondgeneration sequencing data. Briefings in Bioinformatics 14:193–202. https://doi.org/10.1093/bib/bbs012
- Waterhouse A, Bertoni M, Bienert S, Studer G, Tauriello G, Gumienny R, Heer FT, de Beer TAP, Rempfer C, Bordoli L, Lepore R, Schwede T. 2018. SWISS-MODEL: homology modelling of protein structures and complexes. Nucleic Acids Res. 46:W296–W303. https://doi.org/10.1093/ nar/qky427
- Holm L. 2022. Dali server: structural unification of protein families.
   Nucleic Acids Res. 50:W210–W215. https://doi.org/10.1093/nar/gkac387
- Emsley P, Lohkamp B, Scott WG, Cowtan K. 2010. Features and development of coot. Acta Crystallogr D Biol Crystallogr 66:486–501. https://doi.org/10.1107/S0907444910007493
- Otify AM, Mohamed OG, El-Amier YA, Saber FR, Tripathi A, Younis IY.
   2023. Bioherbicidal activity and metabolic profiling of allelopathic metabolites of three cassia species using UPLC-qTOF-MS/MS and molecular networking. Metabolomics 19:16. https://doi.org/10.1007/s11306-023-01980-5
- Chambers MC, Maclean B, Burke R, Amodei D, Ruderman DL, Neumann S, Gatto L, Fischer B, Pratt B, Egertson J, et al. 2012. A cross-platform toolkit for mass spectrometry and proteomics. Nat Biotechnol 30:918– 920. https://doi.org/10.1038/nbt.2377
- Nothias L-F, Petras D, Schmid R, Dührkop K, Rainer J, Sarvepalli A, Protsyuk I, Ernst M, Tsugawa H, Fleischauer M, et al. 2020. Feature-based molecular networking in the GNPS analysis environment. Nat Methods 17:905–908. https://doi.org/10.1038/s41592-020-0933-6

- Pluskal T, Castillo S, Villar-Briones A, Orešič M. 2010. MZmine 2: modular framework for processing, visualizing, and analyzing mass spectrometry-based molecular profile data. BMC Bioinformatics 11:1–11. https:// doi.org/10.1186/1471-2105-11-395
- Shannon P, Markiel A, Ozier O, Baliga NS, Wang JT, Ramage D, Amin N, Schwikowski B, Ideker T. 2003. Cytoscape: a software environment for integrated models of biomolecular interaction networks. Genome Res. 13:2498–2504. https://doi.org/10.1101/gr.1239303
- van Santen JA, Jacob G, Singh AL, Aniebok V, Balunas MJ, Bunsko D, Neto FC, Castaño-Espriu L, Chang C, Clark TN, et al. 2019. The natural products atlas: an open access knowledge base for microbial natural products discovery. ACS Cent Sci 5:1824–1833. https://doi.org/10.1021/ acscentsci.9b00806
- 99. van Santen JA, Poynton EF, Iskakova D, McMann E, Alsup TA, Clark TN, Fergusson CH, Fewer DP, Hughes AH, McCadden CA, Parra J, Soldatou S, Rudolf JD, Janssen EM-L, Duncan KR, Linington RG. 2022. The natural products atlas 2.0: a database of microbially-derived natural products.

- Nucleic Acids Res. 50:D1317–D1323. https://doi.org/10.1093/nar/gkab941
- Böcker S, Letzel MC, Lipták Z, Pervukhin A. 2009. SIRIUS: decomposing Isotope patterns for metabolite identification. Bioinformatics 25:218– 224. https://doi.org/10.1093/bioinformatics/btn603
- Dührkop K, Nothias L-F, Fleischauer M, Reher R, Ludwig M, Hoffmann MA, Petras D, Gerwick WH, Rousu J, Dorrestein PC, Böcker S. 2021.
   Systematic classification of unknown metabolites using high-resolution fragmentation mass spectra. Nat Biotechnol 39:462–471. https://doi.org/10.1038/s41587-020-0740-8
- Allaire JJ. 2015. RStudio: integrated development environment for R. RStuiod, Inc., Boston.
- 103. Wickham H. 2011. ggplot2. WIREs Computational Stats 3:180–185. https://doi.org/10.1002/wics.147
- 104. Kassambara A. 2020. ggpubr: "ggplot2" based publication ready plots. Available from: https://cran.r-project.org/web/packages/ggpubr/index. html. Retrieved 15 Jan 2021.